Available online www.jsaer.com

***Journal of Scientific and Engineering Research*, 2018, 5(2):400-408**

Research Article

ISSN: 2394-2630
CODEN(USA): JSERBR

Study of the Intraparticle Diffusion of Cr (VI), Mn (II) and Cd (II) on Modified Gold Coast Bombax

Musah M*[1], Yerima H[1], Haruna B[1], Musa A[2], Umar MT[3]

[*1]Department of Chemistry, Niger State College of Education, Minna, Nigeria
[2]Department of Chemistry, Umaru Musa Yar'Adua University, Katsina, Nigeria
[3]Department of Chemistry, Ibrahim Badamasi Babangida University, Lapai, Nigeria

Abstract In this study, activated carbons were prepared from calyx of Gold coast bombax through the two step activation process using sulphuric acid and potassium hydroxide as activating agents. The activated carbons were functionalized using nitric acid. The functionalized carbons were characterized by X-ray defractometer, zetasizer and pH meter. The carbons showed intense x-ray diffraction peaks at 2θ values of 24.67^o and 24.47^o respectively. pH zero point of charge values of 6.40 and 6.60 were obtained and were lower than pH values of 7.01 and 6.93. Mckay and Poots; and Weber and Morris intraparticle diffusion gave relatively low correlation coefficients. Results indicate the suitability of the functionalized activated carbons in the adsorption of Cr (VI), Mn (II) and Cd (II); and the process is not entirely intraparticle diffusion controlled.

Keywords Heavy metals, Toxicity, Intraparticle diffusion, Adsorption, Activated carbon

Introduction

The applications of metals and their compounds to any nation's industrial and technological advancement have become very important and indispensable. Pollution derived from these metals has continued to increase as industrial activities increases and metals released from industrial activities into the environment have become real threat to human and animal health [1-2]. Heavy metals are among pollutants of concern that are not subject to degradation or bacterial breakdown [3] and when released into the environment can remain for decades and upon ingestion above tolerable levels can have very harmful effects on human health causing various diseases and disorder [1, 4]. Despite the adverse effects of heavy metals on the environment and human health, exposure to these metals has continued to increase. These metals of concern include chromium, manganese and cadmium. Several researches have reported the presence of toxic heavy metals in industrial wastewater released into the environment, in surface and underground water [5-7].

Recently, the use of activated carbon prepared from agricultural wastes for removal of toxic metals from solutions has been emphasized as it is considered to be cheap, without sludge or precipitate formation and is effective for adsorption of heavy metals even at trace quantities. Activated carbon are highly developed carbonaceous materials with porous structure produced through carbonization and subsequent activation of the material by chemical or physical process [8]. Activated carbon can be functionalized to enhance their adsorptive capacities. Functionalization involves the oxidation and grafting onto the surface of activated carbon in other to introduce functional groups [9].

Preparation of Activated Carbon

Five (5) grams of carbonized samples was mixed with 5 cm^3 of activating agent (1M H_2SO_4). The samples were then allowed to stand for 2 hours and then introduced into a furnace and heated at 600^{o}C for 20 minutes

(resident time). The activated samples were quenched in iced water then washed with 0.1 M HCl to remove surface ash, followed by hot water and rinsing with distilled water to remove residual acid. Washing of the samples was completed when pH of the supernatant was between 6-8 and then dried in an oven at 105^{o}C overnight before being grounded and stored in air tight containers. The activated carbon (AC) produced was labelled HAC. The same process of activation was repeated using 1M KOH as activating agent. The resultant AC was labelled KAC.

Preparation of Functionalized Activated Carbon

Ten grams each of the activated carbons (HAC and KAC) were suspended separately in 300 cm^3 of 32.5% (v/v) nitric acid solution under stirring and heating at 60 ^{o}C for 5 hours. The mixtures were then filtered, thoroughly rinsed with plenty of distilled water until pH of cleansing water was neutral, then dried in oven at 80 ^{o}C for 8 hours [10].

Characterisation of Activated Carbon

Standard methods of analysis as illustrated below were used for characterization of the activated carbons.

Measurement of pH

In determining pH of the activated carbon method was used. One (1) gram of the sample was weighed into three separate beakers and 20 cm^3 of distilled water was added to each. The samples were macerated with glass rod until the samples became uniformly wetted. The water quantity was increased to 100 cm^3, then stirred for 30 seconds and allowed to stand for one hour. The beakers were covered with a clean watch – glass within the period. After then, the samples were stirred again and 10 cm^3 of the extracts decanted into another clean, dried beaker. The pH was determined using a pH meter at room temperature.

Bulk Density of the Activated Carbon

Three (3) grams of the sample was placed in a graduated cylinder and tapped on bench until the volume of the sample stopped decreasing. The displaced volume was recorded and bulk density calculated as (Sugumaran *et al.*, [11]) as:

P = mass immersed/volume displaced

Measurement of pH Point of Zero Charge

The zero surface charge of the activated carbon characteristics was determined using the salt addition method [12]: Two (2) grams of the adsorbent sample was weighed and transferred into ten different 50 cm^3 beakers and 20 cm^3 of distilled water was added to each beaker. Their pH were adjusted to 2, 3, 4, 5, 6, 7, 8, 9, 10 and 11 using 0.1 M HCl or 0.1 M KOH, and allowed to stand for four days with occasional stirring, after which the pH was recorded as pH_i followed by addition of 0.5 cm^3 2 M NaCl and stirred for 3 hours. After this time, the pH was read and recorded as pH_f. The change in pH ($\Delta pH = pH_f - pH_i$) was calculated and the graph of ΔpH versus pHi was plotted.

X-Ray Diffraction

X-Ray Diffraction analysis was carried out with Rigaku X-Ray Diffractometer [Ultima III] for the samples under identical conditions with CuKα radiation whose wavelength (λ) = 1.54 Å, tube voltage is 40 kV, and tube current is 30 mA. Scan Range: 10^{o}– 80^{o}, Scan Mode: Continuous and Speed: 5^{o}/min.

Particle Size Analysis (DLS Techniques)

The particle size and hydrodynamic diameter was determined using Zetasizer Nano S at scattering angle of 173^{o} operating at 25 ^{o}C with equilibrating time of 10 sec per runs. 1 mg of each sample was dispersed in 10 dm^3 of distilled water by means of a sonication and a centrifugation at 3000 rpm 5 min. The supernatant (free of larger aggregates) was then transferred into a polystyrene quartz cuvette using a syringe with 0.23 μm filter and placed in the Zetasizer Nano S cuvette holder immediately for analysis.

Batch Adsorption Studies

The batch adsorption method was used where 0.2 g of activated carbon was interacted with 20 cm^3 of adsorbate solutions. This was allowed to shake for 30 minutes at 250 rpm. The process was repeated at 60, 90, 120 and 150 minutes for the solution studied. The mixture was filtered separately using Whatman filter paper (No. 42) and filtrate collected into sample bottles [13-14]. Concentrations of heavy metal ions in the solution were determined before and after interactions with activated carbon using Atomic Absorption Spectrophotometer and the removal efficiency (%) was calculated as:

$$\text{RE (\%)} = \frac{(C_o - C_f) \times 100}{C_o} \quad (1)$$

Where:

Co is concentration of heavy metal ion before interaction with activated carbon

C_f is concentration of heavy metal ion after interaction with activated carbon

Adsorption capacity at time t (q_t) was calculated as:

$$q_t = \frac{(C_o - C_t)\, v}{m} \quad (2)$$

Where:

v is volume of aqueous solution used for interaction

m is mass of adsorbent used

Physico-chemical Properties of the Adsorbents

Results of the physico-chemical Properties of H_2SO_4 Modified Activated Carbon (HAC) and KOH Modified Activated Carbon (KAC) are presented in Table 1. pH values of 7.88±0.00 and 8.21±0.01 were obtained for HAC and KAC before been functionalized. Near neutral pH values of 7.01±0.13 and 6.93±0.07 were obtained in HAC and KAC respectively. The activated carbons had different bulk densities, with HAC having the highest (0.79±0.04 g/cm^3) followed by KAC (0.53±0.04 g/cm^3).

Table 1: Selected Properties of Functionalized Activated Carbons

Parameter	HAC	KAC
pH	7.01±0.13	6.93±0.07
Bulk density (g/cm^3)	0.79±0.04	0.73±0.03

Key: HAC = H_2SO_4 Modified Activated Carbon (Functionalized);
KAC = KOH Modified Activated Carbon (Functionalized)

Bulk density is the property granules, powdered and other form forms divided materials expressed by the mass of the particles divided by total volume occupied. The total volume includes pore volume, intra-particle void volume and particle volume of the material. Bulk density of activated carbons also depends on the nature of the starting material and process of preparation [15]. This property determines the ability of activated carbon to retain liquid and helps determine the compressibility of the activated carbon [16].

Results of bulk density indicate that HAC had higher bulk density (0.79±0.04 g/cm^3) while KAC had 0.73±0.03 g/cm^3. These values are higher than the 0.33±0.00 g/cm^3 and 0.34±0.00 g/cm^3 obtained for banana empty fruit bunch and *Delonix regia* fruit pod activated carbons respectively [11] but similar to 0.72 g/cm^3 obtained for *Balsamodendron caudatum* wood activated carbon [17].

Elemental Composition of the Calyx of Gold coast bombax, HAC and KAC

Figure 1 present the elemental compositions of HAC, KAC and BBCx expressed in percentage of dry weight. The result showed 87.02%, 77.46% and 61.04% carbon; 2.06%, 2.31% and 0.34% calcium in HAC, KAC and BBCx respectively. Magnesium was present in HAC and KAC at 0.92% and 1.47% while potassium was only present in KAC. The elemental composition of the Calyx of Gold coast bombax revealed the presence of carbon, oxygen and calcium at 61.04, 38.62 and 0.34% respectively. Carbon and oxygen content obtained are higher than the 59.4% and 35.3% obtained for reed black [18]. The carbon content is also higher than 41.75% and 34.22% reported for Banana empty fruit bunch and *Delonix regia* fruit pod whose oxygen values (51.73% and

58.91%) are higher than the 38.62% for BBCx. These values indicate that BBCx is a good precursor for production of activated carbon. Carbon content in HAC and KAC were higher than the 73.09% reported for activated prepared from used tea bags [19].

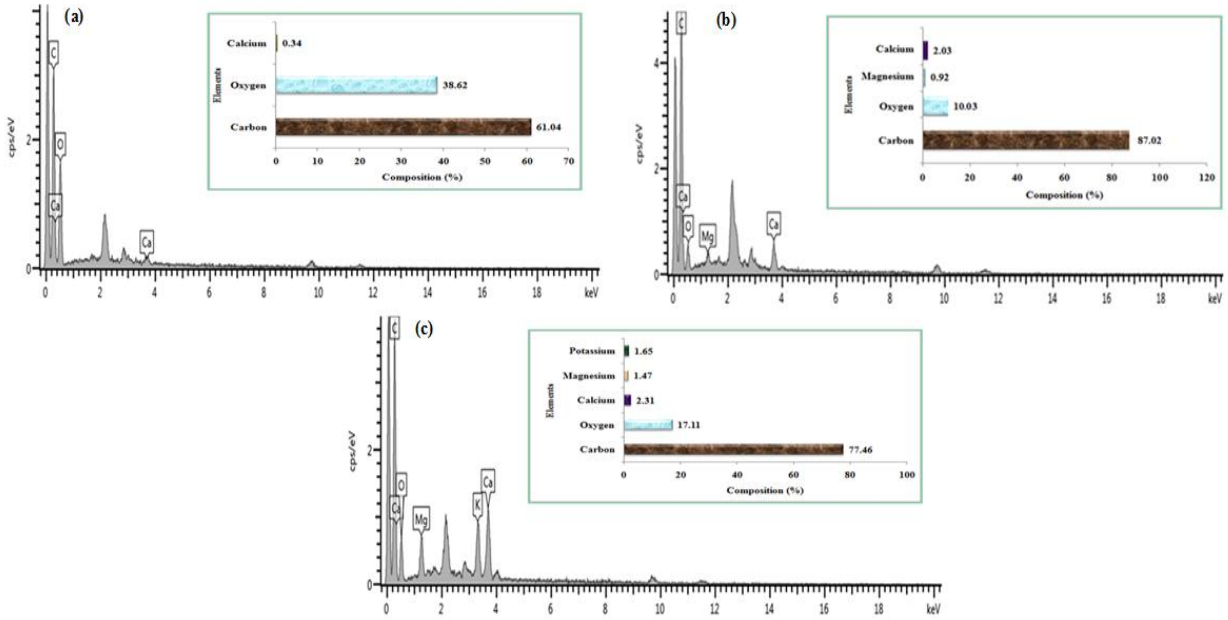

Figure 1: EDS Spectra of (a) Calyx of Gold coast bombax (BBCx) (b) H_2SO_4 modified activated carbon (HAC) (c) KOH treated activated carbon (KAC)

pH Zero Point of Charge (pHzpc)

Figure presents the pH zero point of charge (pHzpc) for HAC and KAC respectively. The pHzpc of an adsorbent is the pH value at which the sorbent exhibits zero net electrical charge on the surface when submerged into an electrolyte [12, 20]. It helps provide understanding of the mechanism of sorption [21]. The value of pH is used to describe pzc only for systems in which H^+/OH^- are the potential-determining ions. When pH is lower than the pzc value (pH < pHpzc), the adsorbent surface is positively charged, hence attracting anions. At pH greater than pzc (pH > pHpzc), the adsorbent surface is negatively charged thereby increasing the electrostatic attraction between positively charged adsorbate and adsorbent particles [21-22].

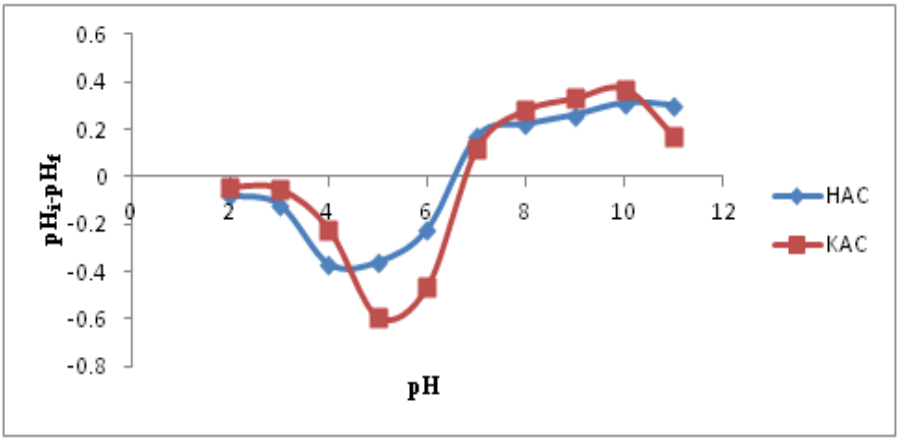

Figure 2: pH Point of Zero Charge of (a) H_2SO_4 modified activated carbon (HAC) (b) KOH modified activated carbon (KAC)

pHpzc values obtained for HAC and KAC are 6.40 and 6.60 respectively. These can be interpreted as pH > pHpzc for HAC and KAC (7.01 > 6.40 and 6.93 > 6.60). The adsorbent surfaces are negatively charged owing to the presence of OH^- group, a situation that favours the adsorption of Cr^{6+}, Mn^{2+} and Cd^{2+}. Similar observation was reported in the adsorption of Zn^{2+} onto bentonite clay [23].

X-Ray Diffractions (XRD) of Adsorbents

The XRD spectra activated carbon provides information on the crystalline or amorphous nature of the sorbent [21]. The XRD spectra of HAC and KAC are presented in figure 3. The spectra of HAC showed sharp and intense peak at 2θ value of 24.67^o with other low intensity peaks at 2θ equal to 26.72^o, 31.04^o, 44.33^o and 47.91^o; sharp intense peak at 2θ equals 24.47^o and low peaks at 26.41^o, 39.32^o, 44.26^o, 48.67^o and 50.06^o occurred in KAC. The sharp and intense peaks at 2θ equal to 24.67^o and 24.47^o with low intensity peaks around 44^o in the spectra of HAC and KAC indicate the presence of organised crystalline structure of graphitic carbon [24] which is due to high lignin or low hemicelluloses content in the precursor [8] and this also correspond to the planes of orientation of (002) and (100) respectively [25-26].

It can be seen from figure 3 that there is no significant difference in the major peaks in the XRD patterns of HAC and KAC suggesting that the chemical activation process did not create a major difference in the microstructure of HAC and KAC as seen in the position of their sharp and intense peaks.

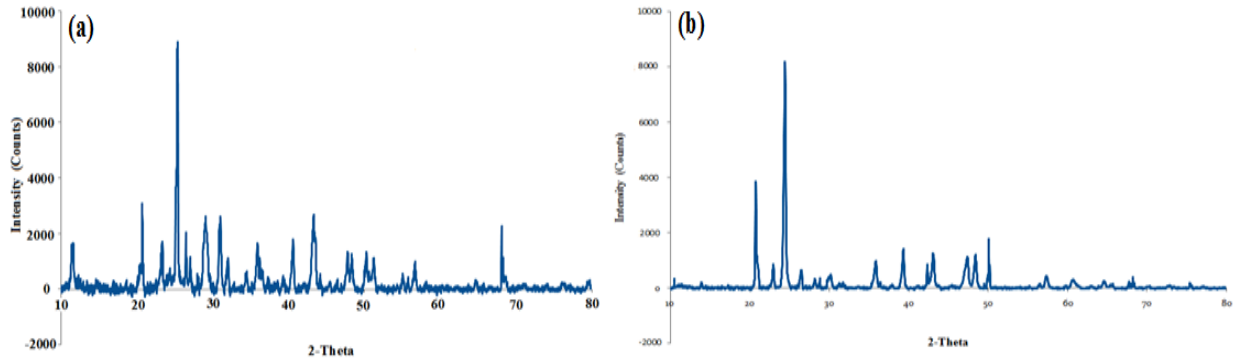

Figure 3: XRD Spectra of (a) H_2SO_4 modified activated carbon (HAC) (b) KOH modified activated carbon (KAC)

The crystalline structural arrangement of the activated carbons increases the adsorption of metal ions onto the surface of the adsorbent [27]. Elkady *et al.* [25] reported that increase in temperature of carbonization will promote the growth of graphitic micro-crystallite and sharpens the peaks of the resultant activated carbon.

Particle Size of HAC and KAC

Figure 4 present the hydrodynamic diameter (D_h) of HAC and KAC. The D_h values were used in determining the diameter, length and aspect ratio of the activated carbons.

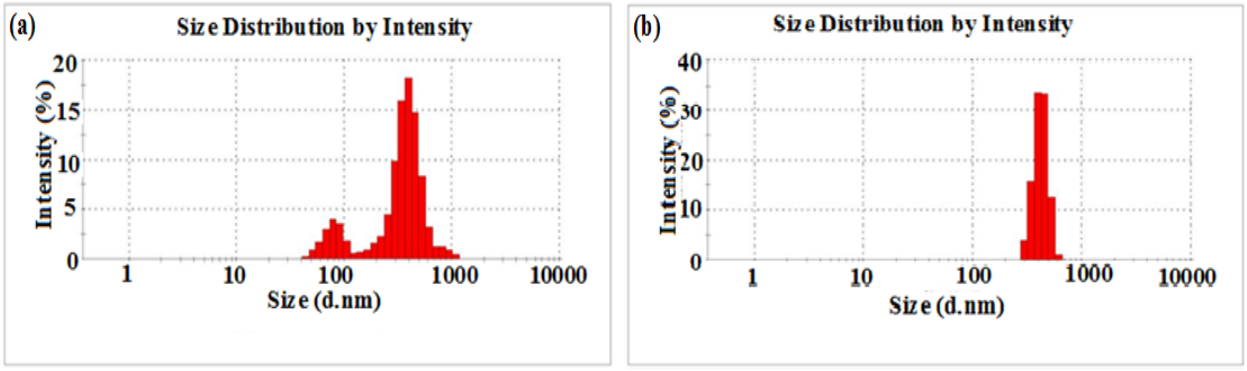

Figure 4: Particle Size Distribution of (a) HAC Particles (Z-Average (d.nm) = 939.4) (b) KAC Particles (Z-Average (d.nm) = 1079)

Aspect ratio was investigated by establishing Dynamic Light Scattering (DLS) Correlation chart. This was achieved by relating the diameter of HAC and KAC obtained from their X-Ray spectra with the hydrodynamic diameter ($D_{h)}$ using the modified Navier-Stokes equation and Stokes-Einstein equations expressed as Equations (3) and (4) respectively. The chart is aimed at determining the aspect ratio and length at a specific diameter of HAC and KAC.

$$D = \frac{kT}{3\pi\eta L}\left[In\left(\frac{L}{d}\right) + 0.32\right]$$

(3)

$$D = \frac{kT}{3\pi\eta D_h}$$

(4)

where D is the diffusion coefficient, k is the Boltzmann constant, T is temperature, η is the viscosity, D_h is the hydrodynamic diameter, and "L" and "d" are the length and diameter of the activated carbons respectively. Combining the equations relates D_h to the dimensions of the activated carbons in the form of Equation (5):

$$D_h = \frac{L}{In\left(\frac{L}{d}\right)+0.32}$$

(5)

The hydrodynamic diameters of HAC and KAC obtained from DLS Nanosizer were 939.4 nm and 1079 nm nm respectively. The developed correlation chart is presented in Figure 4(b).

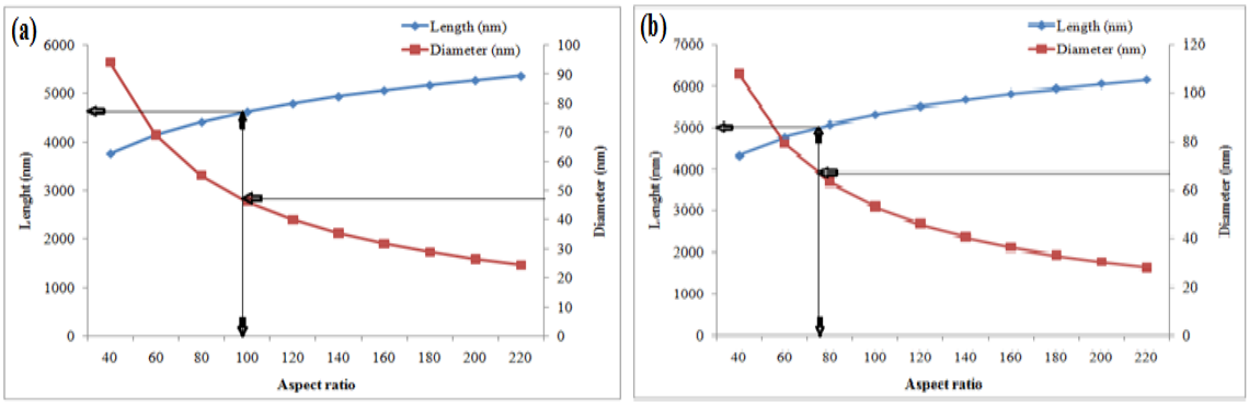

Figure 5: Aspect ratio, Diameter and Length of (a) HAC (b) KAC

The correlation charts presented in Figure 5 showed high aspect ratio value for HAC (97.68) compared to 78.10 obtained for KAC. Diameter (68.50 nm) and length (4954.35 nm) were obtained for KAC and are higher than 47.30 nm (diameter) and 4602.39 nm (length) for HAC. These values justify the low aspect ratio of HAC.

McKay and Poots Intraparticle Diffusion Model

The model is used to establish the mechanism of adsorption process. According to the model, plot of uptake, q_t versus square root of time ($t^{1/2}$) should give a linear line if intraparticle diffusion is involved in the sorption process [3]. The McKay and Poots equation is expressed as [28]:

$$q_t = K_1 t^{1/2} + X^1 \quad (6)$$

Where K_1 is the intraparticle diffusion rate constant (mg/gmin$^{1/2}$) and X^1 is the boundary layer diffusion effect.

Values of K_1 and X^1 presented in Table 2 were obtained from the slope of the plot of qt versus $t^{1/2}$ for adsorption of Cr^{6+}, Mn^{2+} and Cd^{2+} onto HAC and KAC. The initial curves in the plots are due to boundary layer diffusion effects and an extrapolation of the linear line to the time axis gives the intercept, X^1 which is proportional to the thickness of the boundary layer [3]. Boundary layer gives indication of the ability of the adsorbents to remove ions from solution and is also seen as viscous drag which exists between the sorbent surface and solution containing metal ions diffusing across the boundary layer [28].

X^1 values obtained for adsorption Cr^{6+} onto HAC and KAC presented in Table 2 are 0.661 and 0.519 mg/g. Those of Mn^{2+} adsorption are 0.425 and 0.502 mg/g respectively. The higher the X^1 value the greater the boundary thickness and indicate higher adsorption capacity [3]. From the results, the boundary layer thickness varies between 0.661 and 0.425 mg/g with the adsorption of Cr^{6+} onto HAC having the highest X^1 value (0.661 mg/g) indicating high adsorption capacity for Cr^{6+}. The value (0.661 mg/g) is higher than 0.167, 0.039 and 0.091 mg/g reported for adsorption of Strontium onto rice straw activated carbon [29] but lower than 0.894 mg/g obtained for removal of lead by Youssef *et al.* (2013). The thickness of a boundary layer decreases as temperature increases and this

increases the tendency of the ions to escape from the adsorbent surface to the solution phase resulting in a decrease in adsorption [3, 30].

Table 2: Intraparticle diffusion model experimental constants for adsorption of Cr^{6+}, Mn^{2+} and Cd^{2+}

Kinetic Model	Parameter	Cr^{6+}		Mn^{2+}		Cd^{2+}	
		HAC	KAC	HAC	KAC	HAC	KAC
McKay and Poots	R^2	0.678	0.626	0.664	0.841	0.835	0.576
Intraparticle	k^1 (mg/gmin$^{1/2}$)	0.026	0.038	0.039	0.040	0.031	0.028
diffusion	X_1 (mg/g)	0.661	0.519	0.502	0.474	0.599	0.615
Weber and Morris	R^2	0.776	0.728	0.759	0.897	0.835	0.684
Intraparticle	k_{id}(mg.g^{-1}min^{-1})	0.489	0.327	0.316	0.313	0.426	0.429
diffusion	n	0.278	0.441	0.459	0.453	0.335	0.325

Correlation coefficient (R^2) values close to 1 indicate a good fit of model to experimental data [13] but low R^2 values (0.576 – 0.856) were obtained (as seen in Table 2) for adsorption of $Cr^{6+}$and Mn^{2+} suggesting that the model did not give a good fit with the experimental data hence the process is not entirely intraparticle diffusion controlled.

Weber and Morris Intraparticle Diffusion Model

To further study the intraparticle diffusion process of the adsorption of Cr^{6+}, Mn^{2+} and Cd^{2+} onto HAC and KAC, Weber and Morris model was used. The linear form of the model is expressed as:

$$\log q_t = \log K_{id} + n \log t \quad (7)$$

where K_{id} is the intraparticle diffusion rate constant and n depicts the mechanism of sorption. Values of K_{id} and n values are presented in Table 2. The intrparticle diffusion rate constant, K_{id} obtained range from 0.277 to 0.489 mgg^{-1}min^{-1} for Cr^{6+}, Mn^{2+} and Cd^{2+}, while n values are between 0.278 and 0.514 respectively. Intraparticle diffusion rate constant, K_{id} gives an idea about the thickness of the boundary layer [31]. The larger the K_{id} value the greater will be the effect of the boundary layer and an increase in the rate of adsorption [32-33]. The low values of K_{id} on Table 2 indicate the presence of intraparticle diffusion process as one the rate determining steps among other processes controlling the rate of sorption which may also be operating simultaneously [28]. The 0.426 mgg^{-1}min^{-1} obtained in the sorption of Cd^{2+} onto HAC is closed to the 0.445 mgg^{-1}min^{-1} reported for the removal of Cd^{2+} [34] but higher than the 0.0882 mgg^{-1}min^{-1} obtained for the adsorption of titanium [35]. High n-values suggest better adsorption mechanism [28]. n-values obtained (0.459 and 0.453) for adsorption of Mn^{2+} onto HAC and KAC are higher than 0.0048, 0.0068 and 0.0125 reported for adsorption of Pb^{2+}, Cd^{2+} and Cu^{2+} by modified cocoa pod husk [3].

The low correlation coefficients (R^2) of Weber and Morris intraparticle diffusion which are similar to those of McKay and Poots model also confirm that intraparticle diffusion is not the only rate determining process. This is observation is similar to reports of Javadian *et al.* [34] and Youssef *et al.* [36] on the adsorption of Cd^{2+} and U^{6+} respectively.

Conclusion

Modification of the activated carbons with nitric acid showed improved properties. The low pHzpc compared to the pH, high pore content depicted by the XRD spectra and high bulk density indicate the suitability of the activated for adsorption of cations from wastewater.

Acknowledgement

Authors deeply appreciate Departments of Chemical Engineering and Chemistry of Ahmadu Bello University Zaria and Niger State College of Education, Minna, Nigeria for allowing the use their facilities

References

[1]. Azizi, S., Kamika, I. & Tekere, M. (2016). Evaluation of heavy metal removal from wastewater in a modified packed bed biofilm reactor. *PLoS ONE*, 11(5):1-13.

[2]. Orjuela, J. P. & Gonzalez, A. (2011). Model of heavy metals adsorption system using the S-Layer of *Basillus spaericus*. Proceeding of the 2011 COMSOL Conference, Boston

[3]. Odoemelam, S. A., Iroh, C. U. & Igwe, J. C. (2011). Copper (II), cadmium (II) and lead (II) adsorption kinetics from aqueous metal solutions using chemically modified and unmodified cocoa pod husk (*Theobroma cacao*) waste biomas. *Research Journal of Applied Sciences,* 6(1):44-52.

[4]. Li, H., Xiao, D., He, H., Lin, R & Zuo, P. (2012). Adsorption behaviour and adsorption mechanism of Cu (II) ions on amino-functionalized magnetic nanoparticles. *Transactions of Nanoferrous Metals Society of China*, 23:2657-2665

[5]. Singh, N. & Gupta, S. K. (2016). Adsorption of heavy metals: A review. *International of Innovative Research in Science, Engineering and Technology*, 5(2):2267-2281

[6]. Idris, S., Ndamitso, M. M., Mohammed, E. B. & Labade, T. O. (2013). Adsorption kinetics of the removal of biochemical oxygen demand (BOD) from dye effluent onto poultry droppings activated carbon. *British Journal of Applied Science & Techchnology*, 3(3):628-637.

[7]. Anyakora, C., Nwaeze, K., Awodele, O., Nwadike, C., Arbabi, M. & Coker, H. (2011). Concentrations of heavy metals in some pharmaceutical effluents in Lagos, Nigeria. *J. Environ. Chem. and Ecotoxicology,* 3(2):25-31.

[8]. Isahak, W.N.R.W., Hisham, M.W.M. and Yarmo, M.A. (2013). Hyghly porous carbon materials from biomass by chemical and carbonization method: A comparison study. *Journal of Chemistry.* 1-6. doi.org/10.1155/2013/620346

[9]. Bhatnagar, A., Hogland, W., Marques, M. & Sillanpa, M. (2013). An overview of the modification methods of activated carbon for its water treatment applications. *Chemical Engineering Journal*, 219:449-511.

[10]. Albishri, H. M. & Marwani, H. M. (2011). Chemically modified activated carbon with tris(hydroxymethyl)aminomethane for selective adsorption and determination of in water samples. *Arabian Journal of Chemistry*, doi:10.1016/j.arabjc.2011.03.017

[11]. Sugumaran, P., Priya, S.V., Ravichandran, P. & Seshadri, S. (2012). Production and Characterization of Activated Carbon from Banana Empty Fruit Bunch and *Delonix regia* Fruit Pod. *Journal of Sustainable Energy and Environment*, 3,125-132.

[12]. Cardenas- Pena, A.M., Ibanez, J.G. & Vasquez-Madrano, R. (2012). Determination of the point of zero charge for electrocoagulation precipitates from an iron anode. *International Journal of Electrochemical Science*, 7:6142-6153.

[13]. Musah, M., Yisa J., Mann, A., Suleiman, M.A.T. & Auta, M. (2016). Application of Factorial Design to the Adsorption Cd (II) ion from Aqueous Solution onto Chemically Modified *Bombax buonopozense* Calyx. *Journal of Scientific and Engineering Research*, 3(3):188-193

[14]. Shama, S. A., Moustafa, M. E. &Gad, M. E. (2010). Removal of heavy metals Fe^{3+}, Cu^{2+}, Zn^{2+}, Pb^{2+}, Cr^{3+} and Cd^{2+} from solutions by using *Eichhornia crassipes*. *Portugaliae Electrochimica Acta*. 28(2):125-133.

[15]. Malik, R., Ramteke, D.R. & Wate, S.R. (2006). Physico-chemical and surface characterization of adsorbent prepared from groundnut shell by $ZnCl_2$ activation and its ability to adsorb colour. *Indian Journal of Chemical Technology*, 13:319-3328

[16]. Hebert, V. (2011). Bulk density of powders made easy. Retrieved on 18th June, 2015 from http:/www.brookfieldengineering.com

[17]. Sivikumar, K., Kannan, C. & Karthikeyan, S. (2012). Preparation and characterization of activated carbon prepared from *Balsamodendron caudatun* wood waste through various activation processes. *Rasayan Journal of Chem.*, 5(3):321-327.

[18]. Sun, Y. Zhang. J.P. Yang, G. & Li, Z.H. (2006). Removal of pollutants with activated carbon from K_2CO_3 activation of lignin from reed black liquors. *Chem., Biochem. and Eng.,* 9(20).427-435.

[19]. Shalma. T. & Yogamoorthi, A. (2015). Preparation and characterization of activated carbon from used tea dust in comparison with commercial activated carbon. *International Journal of Recent Scientific Reseach*, 6(2).2750-2755.

[20]. Sumithra, C., Murugavel, S.C. & Karthikeyan, S. (2014). Evaluation of dynamics and equilibrium models for the sorption of basic violet 3 on activated carbon prepared from *Moringa oleifera* fruit shell wastes. *Carbon-Science and Technology*, 6(1),342-348.

[21]. Dawodu, F.A. & Akpomie, .K. G. (2014). Simultaneous adsorption of Ni (II) and Mn (II) ions from aqueous solution onto a Nigeria kaolinite clay. *Journal of Materials Researchand Technology*, 3(2): 129-141.

[22]. Deng, H., Yang, L., Tao, G. & Dai, J. (2009). Preparation and characterization of activated carbon from cotton stalk by microwave assisted chemical activation-Application in mathylene blue adsorption from aqueous solution. *Journal of Hazardous Materials*, 166, 1514-1521. doi:10.1016/j.jhazmat.2008.12.080

[23]. Araujo, A. L. P., Bertagnolli, C., Silver, M. G. C., Gimenes, M. L. & Barres, M. A. S. D. (2013). Zinc adsorption in bentonite clay: Influence of pH and initial concentration. *ACTA Scientiarum*, 35(2):325-332.

[24]. Jeyakumar, R. P. S. & Chandrasekara, V. (2013). SEM, FTIR and XRD studies of the removal of Cu (II) from aqueous solution using marine green algae. *Global Research Analysis*, 2(11):10-13.

[25]. Elkady, M. F., Hussein, M. M. & Salama, M. M. (2015). Synthesis and characterization of nano-activated carbon from elmaghara coal, Sinai, Egypt to be utilized for wastewater purification. *American Journal of Applied Chemistry*, 3(3):1-7.

[26]. Manoj, B. & Kunjomana, A. G. (2012). Study of stacking structure of amorphous carbon by X-ray diffraction technique. *International Journal of Electrochemical Science*, 7:3127-3134.

[27]. Hamza, N. A. E., Hammad, A. Y. & Eltayeb, M. A. (2013). Adsorption of metals (Fe (II), Cr (III) and Co (II)) from aqueous solution by using activated carbon prepared from mesquite tree. *Science Journal of Analytical Chemistry*, 1(2):12-20.

[28]. Patil, S. D., Renukdas, S. & Patel, N. (2012). Comparative study of kinetics of adsorption of methylene blue from aqueous solutions using cinnamon plant (*Cinnamonum zeylanicum*) leaf powder and pineapple (*Ananas comosus*) peel powder. *The Electronic Journal of Chemistry*, 4(2):77-100

[29]. Yakout, S. M. & Elsherif, E. (2010). Batch kinetics, isotherm and thermodynamic studies of adsorption of strontium from aqueous solutions onto low cost rise straw based carbons. *Carbon-Science and Technology*, 1:144-153.

[30]. Itodo, A. U., Abdulrahman, F. W., Hassan, L. G., Maigandi, S. A. & Itodo, H. U. (2010). Intraparticle diffusion and intraparticulate diffusivities of herbicide on derived activated carbon. *Researcher*, 2(2):74-86.

[31]. Ram-Prasath, R., Muthirulam, P. & Kannan, N. (2014). Agricultural wastes as low cost adsorbents for the removal of acid blue 92 dye: A comparative study with commercial actvated carbon. *IOSR Journal of Agriculture and Vetenary Science*, 7(2):19-32.

[32]. Okewale, A. O, Babayemi, K. A., & Olalekan, A. P. (2013). Adsorption isotherms and kinetics models of starchy adsorbents on uptake of water from ethanol-water system. *Int. J. Appl. Sci. Tech.* 3(1):35-42

[33]. Tan, I. A. W. & Hammed, B. H. (2010). Adsorption isotherms, kinetics, thermodynamics and desorption of activated carbon derived from oil palm empty fruit bunch. *Journal of Applied Sciences*, 10:2565-2571.

[34]. Javadian, H., Ghorbani, F. Tayebi, H. and Hosseini, S. M. (2015). Study of the adsorption of Cd (II) from aqueous solution using zeolite-based geopolymer synthesized from coal fly ash; kinetic, isotherm and thermodynamic studies. *Arabian Journal of Chemistry*, 8:837-849.

[35]. Ekwumengbo, P. A., Kagbu, J. A., Nok, A. J. & Omoniyi, K. I. (2010). Kinetics of gamma globulin adsorption onto titanium. *Rasaya Journal of Chemistry*, 3(2):221-231.

[36]. Youssef, A. M., Dawy, M. B., Akland, M. A. & Abou-Elanwar, A. M. (2013). EDTA versus nitric acid modified activated carbon for adsorption studies of lead (II) from aqueous solutions. *Journal of Applied Science Research*, 9(1):897-912.